A Phase Variable Approach for IMU-Based Locomotion Activity Recognition

Harrison L. Bartlett, *Student Member, IEEE*, and Michael Goldfarb, *Member, IEEE*

***Abstract*—Objective: This paper describes a gait classification method that utilizes measured motion of the thigh segment provided by an inertial measurement unit. Methods: The classification method employs a phase-variable description of gait, and identifies a given activity based on the expected curvature characteristics of that activity over a gait cycle. The classification method was tested in experiments conducted with seven healthy subjects performing three different locomotor activities: level ground walking, stair descent, and stair ascent. Classification accuracy of the phase variable classification method was assessed for classifying each activity, and transitions between activities, and compared to a linear discriminant analysis (LDA) classifier as a benchmark. Results: For the subjects tested, the phase variable classification method outperformed LDA when using nonsubject-specific training data, while the LDA outperformed the phase variable approach when using subject-specific training. Conclusions: The proposed method may provide improved classification accuracy for gait classification applications trained with nonsubject-specific data. Significance: This paper offers a new method of gait classification based on a phase variable description. The method is shown to provide improved classification accuracy relative to an LDA pattern recognition framework when trained with nonsubject-specific data.**

***Index Terms*—Classification algorithms, gait recognition, legged locomotion, patient monitoring.**

I. Introduction

HUMAN movement typically entails a variety of periodic locomotion activities including walking, running, stair ascent, and stair descent. Recently, portable and/or wearable devices have started to emerge (e.g., smartphones, wrist monitors, etc.), which are able to monitor human movement and activity. Such monitoring has a number of potential applications, particularly with regard to healthcare. The monitoring of activities can include varying levels of precision. In the simplest form, monitoring may entail a recognition of movement, relative to absence of movement. Monitoring may further entail recognition of the number of steps during movement (e.g., similar to a common pedometer). In addition to number of steps, movement monitoring may provide recognition of activity type, such as walking, stair ascent, or stair descent. In this paper, such monitoring is referred to as activity monitoring (i.e., monitoring the number of steps associated respectively with a set of possible activities). Although various sensing technologies are available for such monitoring, such activity monitoring systems should ideally employ a minimum set of sensors. Due to the recent introduction of low-cost multi-axis MEMS-based inertial measurement units (IMUs), and to the relative ease with which they can be worn, MEMS IMUs are a particularly compelling sensing technology for such applications. As such, this paper offers a methodology for activity monitoring of locomotion activities that incorporates measurements from a single leg-worn IMU.

Given the recent emergence of wearable sensors (e.g., wrist-worn sensors, smartphones, etc.) and the number of potential applications associated with activity monitoring, many researchers have begun developing activity monitoring algorithms. Reviews of various methodologies employed for activity monitoring using body-mounted sensors are given in [1]–[3]. The vast majority of methods described in these reviews, particularly for purposes of gait activity classification, employ pattern recognition approaches. Many variations of pattern recognition approaches exist, but nearly all employ a similar sequential computational taxonomy, which consists of first windowing sensor data; then extracting characteristic features from the windowed data; then potentially reducing the number of features using dimension reduction techniques; and finally employing a classification algorithm or approach to classify the data (in this case into a possible set of locomotion activities). As described in [4], some common features used in the feature extraction component include time-domain features (e.g., mean, median, variance, etc.), frequency-domain features (e.g., mean, median, or variance of frequency content from FFT), and wavelet-based features, which essentially provide an indication of frequency content changes over time. Although this paper does not focus on the relative utility of these feature types, a recent paper by [4] examining the relative accuracy of a gait activity classification approach using various feature types indicated that time and frequency-based feature types yielded higher classification accuracies than wavelet-type features. Regardless, following the feature selection and potential dimensional reduction components of the pattern recognition taxonomy, a classification algorithm is employed to classify activity based on the (full or reduced) set of features. A large number of classification algorithms exist. A partial review of

Manuscript received April 5, 2017; revised July 7, 2017; accepted September 4, 2017. Date of publication September 8, 2017; date of current version May 18, 2018. This work was supported by the National Science Foundation Graduate Research Fellowship Program under Grant 1445197. *(Corresponding Author: Harrison L. Bartlett.)*

H. L. Bartlett is with the Department of Mechanical Engineering, Vanderbilt University, Nashville, TN 37235 USA (e-mail: harrison.l.bartlett@vanderbilt.edu).

M. Goldfarb is with the Department of Mechanical Engineering, Vanderbilt University.

Digital Object Identifier 10.1109/TBME.2017.2750139

relevant algorithms is given in [1]. Among the classification algorithms recently used for gait activity classification include support vector machines [5]–[7], hidden Markov models [8], Gaussian mixture models [9], [10], linear discriminant analysis [11], [12], neural networks and decision tree [7], and logistic regression [13].

This paper presents a novel approach to gait activity classification that can be employed either as a complement to, or as an alternate to, the aforementioned pattern recognition approaches. Specifically, the method proposes a new feature set based on a phase-variable-based coordinate system. In the phase variable construct, the progression of a periodic activity is uniquely characterized by a single phase variable (or potentially by a set of phase variables) [14]–[16]. The phase variable construct has been recently employed in the context of human locomotion in several papers associated with the control of powered lower limb prostheses, including papers by [17]–[20]. Rather than employ a phase variable for purposes of prescribing a control behavior within a given locomotion activity (i.e., [17]–[20]), the authors present here a method that employs the notion of a phase variable as a basis to formulate a phase-variable-based set of features for purposes of gait activity identification. This phase-variable-based set of features could be employed in the feature extraction component of any common pattern recognition approach. Rather than do so in this paper, however, the authors examine the value of phase-variable-based features in a heuristic activity recognition algorithm. The method is described in the context of gait recognition (i.e., classification) of three activities: walking, stair ascent, and stair descent, and employs a single variable as input to the classifier. The sagittal plane motion of the thigh is utilized as the (single) input variable for the classifier, and is provided by a single (six-axis) IMU worn on the thigh. Experimental assessments were performed with seven healthy subjects who performed multiple gait activities, including level walking at three speeds, stair ascent, and stair descent. Classification results were obtained with the proposed approach, and compared to results using a linear discriminant analysis (LDA) pattern recognition approach.

II. Algorithm Description

A. Phase Space

As previously mentioned, the method presented here is based on a phase variable (PV) representation, which requires that the variable input of interest be represented in a phase space (i.e., a signal as a function of its derivative). The methodology presented here further requires that the input variable form a simple closed curve in the phase space. Representation of a signal in a phase space (signal as a function of its derivative) as a simple closed curve requires that the signal be periodic and that each period be characterized by a single global maximum, a single global minimum, and no local extrema as a function of time.

The authors consider here the thigh angle with respect to the inertial reference frame (i.e., with respect to the vertical) in the sagittal plane as the input signal for activity classification. The thigh angle generally requires an integration of the corresponding phase in order to form a simple closed curve [20], and as such is represented here in the integral phase space (i.e., as the locus of points relating the angle to the time-integral of the angle). Specifically, the two dimensions (x and y) of the phase space used in this work are the thigh segment angle with respect to the gravity vector in the sagittal plane and the integral of a mean-subtracted version of this angle:

$$\begin{aligned} x(t) &= \theta_T \\ y(t) &= \int_0^t \left[\theta_T - \text{mean}\left(\vec{\theta}_T\right)\right] dt \end{aligned} \tag{1}$$

where θ_T is the thigh angle input. The bounds of the integral coincide with the beginning and end of a stride (i.e., the integral is reset each stride). The vector notation indicates a vector containing the time-history of a particular signal over the course of a stride (i.e., the mean subtraction of the integral occurs once per stride to allow for stride-to-stride consistency in the phase space). Note that this method of using a subtracted mean integral is the same as that originally proposed and implemented by [20].

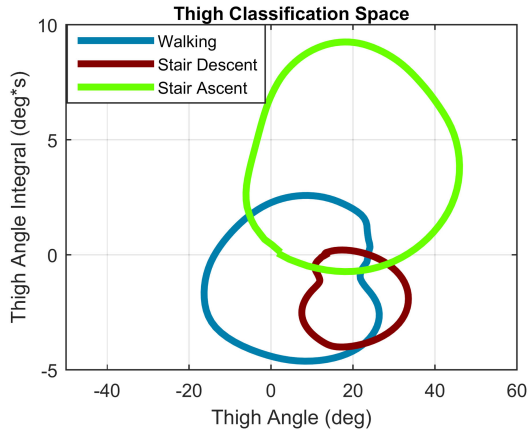

Fig. 1. Phase space for the thigh. The phase space consists of the integral of the mean-subtracted thigh angle plotted against the thigh angle. Thigh angle is calculated relative to the gravity vector in the sagittal plane. Walking (blue), stair descent (red), and stair ascent (green) stride data for healthy subjects form simple closed curves in this space.

Fig. 1 shows the averaged thigh angle for seven healthy subjects for walking, stair ascent, and stair descent, plotted in the angle versus mean-subtracted integral phase space, as measured by a motion capture system. Note that, as required by the method, the locus of points for each activity forms a simple closed curve in this space for each limb segment input.

B. Coordinate Frame Construction

As seen in Fig. 1, the orbit of data for each activity is characterized by a unique shape, relative to the other activities. In order to distinguish each curve from the others, a separate activity-specific coordinate frame is constructed from the measured gait data associated with each activity (i.e., a data-driven coordinate frame). Each coordinate frame consists of two coordinates, here named "progression" and "magnitude," respectively. The progression coordinate is associated with the direction along the phase variable in that it indicates the progression through

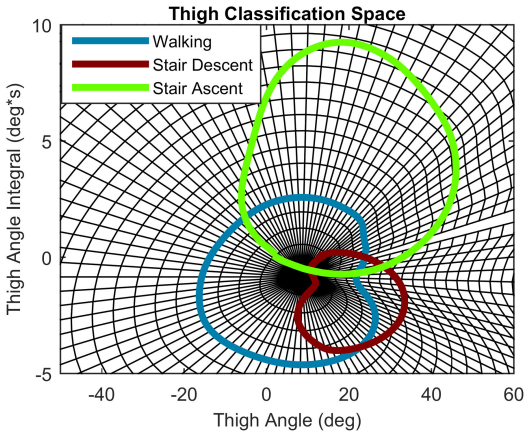

Fig. 2. Custom coordinate frame constructed from a level-ground walking reference curve for the thigh. Walking (blue), stair descent (red), and stair ascent (green) stride data are plotted on this coordinate frame. Each concentric closed curve in the frame is a curve of constant magnitude (m) while each radial line is a line of constant progression (p).

a given stride/period. The magnitude coordinate is the distance from the centroid of the coordinate frame (the origin). Specifically, each activity-specific coordinate frame is established by calculating the centroid of each respective closed activity curve, and using that centroid as the Cartesian origin of the coordinate frame. The centroid-centered curve is then scaled about the origin. This process creates a series of concentric paths (loops of constant magnitude, m) centered about the origin. A series of rays (lines of constant progression, p) are then added which begin at the origin and pass through the reference data points in the phase space. This process creates a "spider web" type shape centered about the origin. It should be noted that reference data that is evenly spaced in time will result in a progression variable p which is also linearly spaced in time.

Fig. 2 shows activity-based coordinate frames created for walking using the thigh angle input. These figures also have superimposed upon them the thigh data associated with walking, stair ascent, and stair descent. For each activity in each activity-specific coordinate frame, the progression and magnitude can be calculated quickly via a coordinate frame transformation, the specific details of which can be found in the appendix:

$$p = f(x, y)$$
$$m = g(x, y) \tag{2}$$

where the progression of a given point is found by interpolating between the progression values associated with each ray in the coordinate frame (i.e., $p = 0$ for the start of a stride and 1 for the end of a stride) by using the angle between the point of interest and the horizontal. The magnitude of a point in the phase space is calculated in the activity-specific coordinate frame as the scalar by which one would need to multiply the original closed curve such that the new closed curve intersected the point of interest in the phase space. Both the progression and magnitude of points in the phase space can be calculated quickly within a given activity-specific coordinate frame.

Using an activity-specific coordinate frame, and given the definitions of progression and magnitude respectively, an instantaneous measure of similarity between an activity and activity-specific coordinate frame can be formed by taking the partial derivative of the magnitude of an activity curve with respect to progression of the curve as follows:

$$D = \frac{\partial m}{\partial p} \tag{3}$$

which is referred to here as the "divergence rate," and denoted by the symbol D. The divergence rate provides an instantaneous measure of how well the local curvature of an activity curve, as a function of progression, matches the activity of the coordinate frame on which it is evaluated. In other words, the divergence rate indicates the extent to which the shape of a curve is aligned with the shape of a given activity-specific coordinate frame. An activity that perfectly matches an activity-specific coordinate frame will have a divergence rate of zero (at all values of progression), regardless of magnitude. A small divergence rate indicates that data in the phase space is concentric with the closed loop used to generate the coordinate frame. Assuming invariance in the shape of an activity curve, as is generally the case in human locomotion, divergence can be used to indicate similarity of shapes shown in Figs. 1 and 2, and thus can be used to identify which activity is being performed. By examining Fig. 2, it can be seen that walking strides are expected to be fairly concentric with the paths of constant magnitude using the walking coordinate frame, yielding low divergence rate (D) values. However, the paths generated by healthy subjects when descending or ascending stairs are not concentric with the paths of constant magnitude in the walking coordinate frame, yielding much higher magnitudes of the divergence rate. This property can be leveraged to classify strides into various activities.

C. Stride Classification

Although Fig. 2 shows only the walking-specific coordinate frame, classification of activity entails constructing activity-specific coordinate frames for each activity, based on training data (i.e., averaged exemplar data). In this study three coordinate frames are constructed – one each for walking, stair descent, and stair ascent, respectively. The reference data used to construct these frames would presumably consist of an average of multiple strides from a single subject, or the average of multiple strides from multiple subjects. Subscripts are used to denote the coordinate frame, where w, d, and a are subscripts that represent the walking, stair descent, and stair ascent coordinate frames respectively.

An activity can be classified by computing the root mean square (RMS) of the divergence rate for a given stride with respect to each activity-based coordinate frame to form a classification vector, $\vec{C}$. This vector, $\vec{C}$, provides a measure of RMS path divergence rate in each activity-based coordinate frame over the course of an entire stride, given by:

$$\vec{C} = \left[RMS(\vec{D}_w) \quad RMS\left(\vec{D}_d\right) \quad RMS(\vec{D}_a) \right] \tag{4}$$

The elements of $\vec{C}$ provide a measure of similarity between the input data and the prototypical reference curve. The

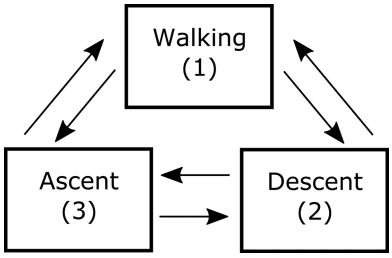

Fig. 3. Activity classification state machine diagram in which each state/activity can transition to any other state/activity. Each state transition is governed by its own transition threshold as described by (7).

current activity can thus be classified as that corresponding to the smallest element of the classification vector.

D. Confidence-Based Hysteretic Switching

The proposed method can also provide a measure of the confidence of gait activity classification by examining the relative magnitudes of the entries in the classification vector, $\vec{C}$. A high degree of confidence is indicated when the magnitude of one entry is much lower than the other entries, while a low confidence is indicated when the entries of $\vec{C}$ are similar in magnitude. The average classifier confidence can be assessed while a user is performing a known activity by averaging the activity-normalized classification vectors across all strides in which the user is performing the known activity:

$$\bar{C}_n = \text{mean}\left(\frac{\vec{C}}{RMS(\vec{D}_n)}\right) \tag{5}$$

where the mean is taken across all strides associated with activity *n*. A classifier confidence matrix, ε, can then be constructed by concatenating the mean classification vectors across all activities into a single matrix (in this case of three activities, this matrix will be 3×3).

$$\varepsilon = \begin{bmatrix} \bar{C}_w \\ \bar{C}_d \\ \bar{C}_a \end{bmatrix} \tag{6}$$

To improve the classification accuracy, a state-machine can be implemented in which the classifier can classify the measured data as one of three states/activities. Each state/activity transitions to any other state/activity through a state transition (Fig. 3). The accuracy of the classifier can be improved by leveraging information from the confidence matrix, ε, in the design of the state transitions. Specifically, a state transition requirement can be constructed from the elements of ε and the measured data such that the classifier will switch from activity *i* to activity *j* if and only if the switching condition is satisfied (where the *i* and *j* numerical indices coincide with the numerical indices indicated for each activity in Fig. 3):

$$\begin{aligned} &\text{switch if } (T_{i\to j})\, RMS\left(\vec{D}_j\right) < RMS\left(\vec{D}_i\right) \\ &T_{i\to j} = S\varepsilon_{j,i} \end{aligned} \tag{7}$$

where $T_{i\to j}$ is a switching threshold gain for the transition between activity *i* and activity *j*, S is a scalar switching sensitivity gain ($S = 0.02$ in this work), and $\varepsilon_{j,i}$ is the element in the jth row and ith column of the confidence matrix ε. The switching sensitivity gain used in this work was empirically tuned, as described in the following subsection of this paper. It should be noted that $T_{i\to j} \neq T_{j\to i}$ which results in different switching conditions for each transition in the finite state machine. As such, the classifier is only allowed to switch states/activities if the RMS of the divergence rate for that stride becomes greater than S multiplied by the expected confidence associated with a new activity, when compared to the current activity. In order for the classifier to switch between activities, the classifier must have a sufficiently high level of confidence that the user is performing a different activity before switching to that activity. For example, in the case that a user is descending stairs, if training data suggests that $RMS(\vec{D}_w)$ is expected to be 10 times greater than $RMS(\vec{D}_d)$ ($\varepsilon_{2,1} = 10$), then the classifier will only switch from walking to stair descent if $RMS(\vec{D}_w)$ is at least 20% (i.e., $0.02{*}10$) greater than $RMS(\vec{D}_d)$. In order to ensure that the algorithm cannot switch from the current state to more than one other state simultaneously, hysteretic switching is implemented as a two-step process: 1) identify the activity associated with the minimum entry in $\vec{C}$, and 2) if the state identified by step 1 is different than the current state, evaluate (7) to determine if a state transition should take place.

III. Implementation and Assessment

A. Experimental Protocol

To assess the efficacy of the previously described classification approach, the approach was implemented on data from seven healthy subjects (five men and two women) performing three locomotor activities – level ground walking (at three cadences), stair descent, and stair ascent. The test subjects ranged in age from 24 to 31 years old with an average age of 26.6 years. The study was performed with approval from the Vanderbilt University Internal Review Board (IRB). Each subject walked over level ground for 20 strides at three different cadences (enforced with a metronome): 85, 100, and 115 steps/min (walking speed was not controlled). The subjects also descended 20 stairs and ascended 20 stairs at a self-selected speed.

Thigh angular motion associated with each subject and each activity was measured using an IMU-based motion capture system (Xsens MVN). The motion capture data was utilized to provide global limb segment angles (angles with respect to the gravity vector) in the sagittal plane for the thigh segment, which was in turn used for the classification analysis previously described. All associated computation was implemented in MATLAB.

B. Analysis

The gait classification approach was assessed by using a leave-one-out cross validation in which data from six subjects was utilized to construct a reference curve ("training data"), and stride data from the seventh subject was classified using the

proposed algorithm. This process was repeated such that each subject's data was classified using the remaining subjects' data to construct the reference curve. This cross-validation process produced seven sets of classifier accuracy data which was averaged to assess the proposed method. This analysis represents an application scenario in which a single reference curve or training set may be applied universally to all users (not a subject-specific classifier).

To determine if the accuracy of the algorithm could be improved with subject-specific reference curves, each subject's strides were classified using the mean of their activity-specific gait data as the reference closed curve. The accuracy of the PV classifier was then assessed by calculating the percentage of accurately classified strides. Accuracy data was averaged across all of the subjects.

Although each element in the classification vector nominally corresponds to the RMS of the divergence rate over an entire stride, the classification vectors for the thigh input were calculated using only the final 75% (i.e., $0.25 \leq p \leq 1.0$) of the stride (i.e., the first 25% of each stride was excluded from consideration in all activities due to the relatively large inter-stride variability observed in the thigh input). If not excluded, the high variability in thigh motion specifically associated with the beginning of stair ascent would negatively affect classifier accuracy, which depends on gait consistency. Following computation of the respective classification vectors, the accuracy of the classifier was assessed by calculating the percentage of accurately classified strides for each individual gait activity. In each case, the stride was classified in the class corresponding to the smallest element in the classification vector. In all accuracy calculations, all walking data was considered regardless of cadence to determine if the approach is robust to variations in step frequency.

The accuracy of the PV classifier was compared to a conventional pattern recognition approach using a linear discriminant analysis (LDA) classifier. The LDA classification approach used two time-domain features to classify each stride: thigh segment angle mean and standard deviation. Note that use of these features is recommended by [4], which indicates that these feature types tend to yield high classification accuracies for activity recognition.

A confidence matrix, ε, was created using the all of the data from the leave-one-out cross validation in which the reference curves were not subject-specific. The single confidence matrix was created by averaging the confidence matrix values from the analysis of each subject's data during the leave-one-out cross validation process. This confidence matrix was then utilized to implement the confidence-based switching state machine as described in (7). All strides were re-analyzed using this confidence-based switching in order to determine if this state machine approach could improve classifier accuracy.

If the switching sensitivity gain as described in (7) is too high, the classifier may be resistant to switching states in order to classify a new activity. If this gain is too low, the confidence-based switching will provide no additional benefit over the phase variable approach alone. The switching sensitivity gain was chosen by tuning the gain in order to maximize the classification accuracy on a single subject using subject-specific training data. This gain value was then used in all other applications of the hysteretic switching algorithm. To assess the activity switching aspect of the proposed algorithm, gait activity transitions were simulated by concatenating gait data from steady state activities into a single set of data. All six possible transitions between the three gait activities (see Fig. 3) were simulated in this way and the strides were classified by all three classification algorithms: linear discriminant analysis (LDA), the phase variable classifier (PV), and the phase variable classifier supplemented with the confidence-based switching (PV+CS). Gait transition data was classified using subject-specific training data and non-subject-specific training data via the previously described method of leave-one-out cross validation.

TABLE 1
THREE BY THREE CONFIDENCE MATRIX ASSOCIATED WITH THE LEAVE-ONE-OUT CROSS VALIDATION

Thigh-Based Classification Confidence Matrix (ε)		Coordinate Frame Utilized		
		Walking	Descent	Ascent
Activity Performed	Walking ($\bar{C}_w$)	1	64	167
	Descent ($\bar{C}_d$)	13	1	77
	Ascent ($\bar{C}_a$)	126	133	1

Each row of the confidence matrix was normalized to the entry associated with the activity being performed as noted in (5).

IV. RESULTS

The average confidence matrix (6) calculated from the leave-one-out cross-validation of the experimental data, is given in Table 1. Recall that the confidence of classification is indicated by the relative magnitudes of the off-diagonal terms in the matrix, where higher off-diagonal numbers indicate a greater degree of confidence (larger expected difference in the entries of $\bar{C}$).

The off-diagonal entries in Table 1 are utilized to determine the thresholds for state transitions in the confidence-based state machine (Fig. 3).

The PV classifier accuracy for the leave-one-out cross-validation is shown in Fig. 4, along with the accuracy resulting from the LDA classifier, and with the accuracy resulting from the phase variable approach with confidence-based switching (PV+CS classifier). The accuracy across all seven tested subjects were averaged to produce the bars (means) and error bars (plus and minus one standard deviation) in Fig. 4. The accuracy of the classifiers is segmented into respective accuracies when classifying each individual activity, then averaged into classifier-specific accuracies to determine the average classifier accuracy.

As shown in the plot, the PV classification accuracies for each activity were $99.4 \pm 1.3\%$, $93.8 \pm 10.8\%$, and $100 \pm 0\%$, for level walking, stair descent, and stair ascent, respectively, which resulted in an average classification accuracy of $97.7 \pm 3.5\%$. For the LDA classifier, the classification accuracies for each activity were $99.1 \pm 2.1\%$, $96.4 \pm 9.4\%$, and $92.0 \pm 18.7\%$, for level walking, stair descent, and stair ascent, respectively, while

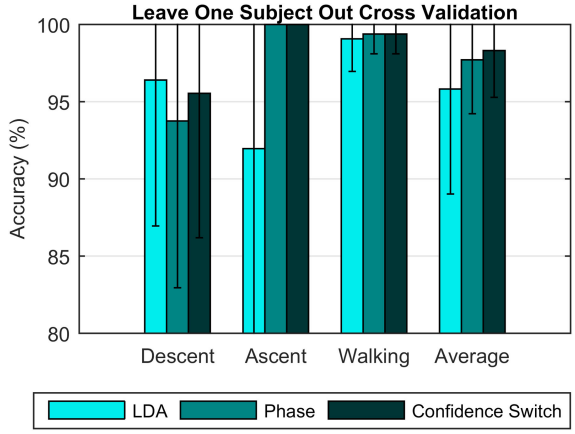

Fig. 4. Classification accuracies from the non-subject-specific training represented by leave-one-out cross validation for the LDA classifier (light blue), phase variable classifier (medium blue), and the phase variable classifier with confidence-based switching (dark blue).

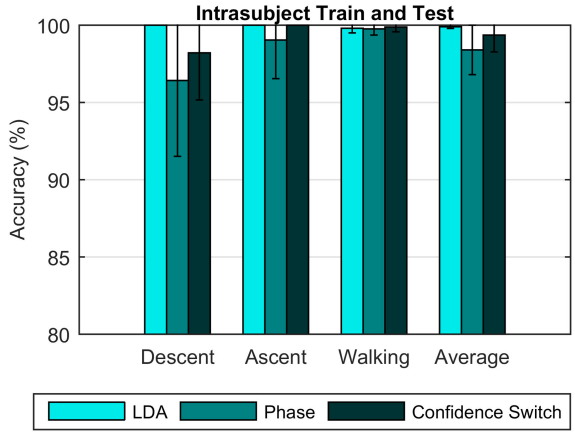

Fig. 5. Classification accuracies from subject-specific training and testing for the LDA classifier (light blue), phase variable classifier (medium blue), and the phase variable classifier with confidence-based switching (dark blue).

the average classification accuracy was 95.8 ± 6.8%. When the phase variable classifier was supplemented with confidence-based switching (PV+CS), the accuracies were 99.4 ± 1.3%, 95.5 ± 9.4%, and 100 ± 0%, for level walking, stair descent, and stair ascent, respectively, while the average classification accuracy was 98.3 ± 3.0%.

The classifier accuracy was also examined using subject-specific reference curves ("training data"). Using subject-specific coordinate frames should account for gait patterns that are unique to individual subjects, and thus should result in higher classification accuracy. The resulting subject-specific classifier accuracies, averaged across all seven subjects are given in Fig. 5. For the PV classifier, the average classification accuracies when using subject-specific frames were 99.8 ± 0.4%, 96.4 ± 4.9%, and 99.0 ± 2.5%, for level walking, stair descent, and stair ascent, respectively, while the average classification accuracy was 98.4 ± 1.6%. For the LDA classifier, the average classification accuracies when using subject-specific frames were 99.9 ± 0.3%, 100 ± 0%, and 100 ± 0%, for level walking, stair descent, and stair ascent, respectively, while the average

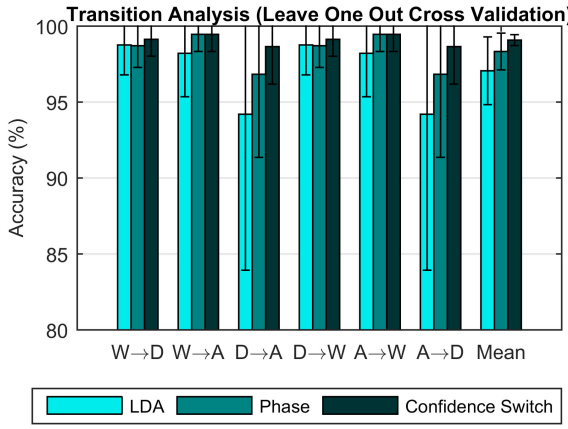

Fig. 6. Classification accuracies for non-subject-specific training for transition gait data (leave one out cross validation) for the LDA classifier (light blue), phase variable classifier (medium blue), and the phase variable classifier with confidence-based switching (dark blue). Transitions from the first activity to the second activity are denoted by arrows where walking, stair descent, and stair ascent are abbreviated by W, D, and A, respectively.

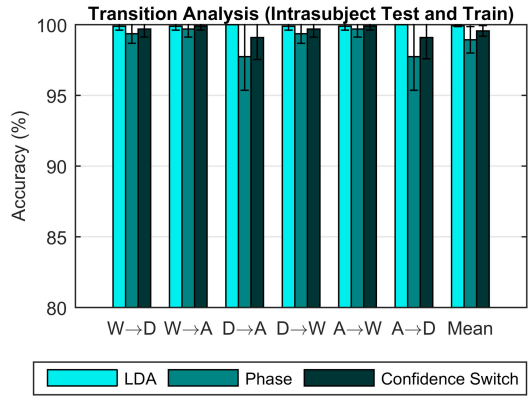

Fig. 7. Classification accuracies for subject-specific training for transition gait data (intrasubject training and testing) for the LDA classifier (light blue), phase variable classifier (medium blue), and the phase variable classifier with confidence-based switching (dark blue). Transitions from the first activity to the second activity are denoted by arrows where walking, stair descent, and stair ascent are abbreviated by W, D, and A, respectively. The mean accuracies across all transition data is additionally presented in the far right set of bars.

classification accuracy was 99.9 ± 0.1%. When the phase variable classifier is supplemented with confidence-based switching (PV+CS), the accuracies were 99.9 ± 0.3%, 98.2 ± 3.0%, and 100 ± 0%, for level walking, stair descent, and stair ascent, respectively, while the average classification accuracy was 99.4 ± 1.1%. Thus, as expected, the accuracy of classification using subject-specific coordinate frames was notably improved relative to the non-subject-specific case (i.e., relative to Fig. 4).

The classifier accuracy was also examined on the concatenated gait data (represented gait transitions) in which all six possible activity transitions were examined. This analysis was performed using non-subject-specific training data via a leave one out cross validation (Fig. 6) and with subject-specific training data (Fig. 7). The classifier accuracies for all the transitions were additionally averaged to more easily compare the classification algorithms.

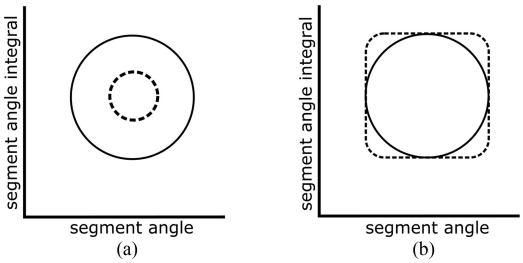

Fig. 8. Example scenario in which two activities plotted in the phase space (solid line activity and dashed line activity) in which LDA should classify more accurately (a) and where the phase variable approach should perform more accurately (b).

V. Discussion

A. Classifier Accuracy

As can be seen from Figs. 4 and 6, the proposed PV classifier (both without and with the confidence-based switching) exhibits higher classification accuracies on average than the LDA classifier while also maintaining more consistent classification accuracies across subjects (i.e., lower standard deviation) when non-subject-specific training data is utilized. In the scenario depicted in Figs. 5 and 7, in which the training data was subject-specific, the LDA classifier outperformed the PV method. As indicated by Figs. 4–7, the addition of confidence-based switching (i.e., PV+CS approach) enhances the classification accuracies relative to the PV approach.

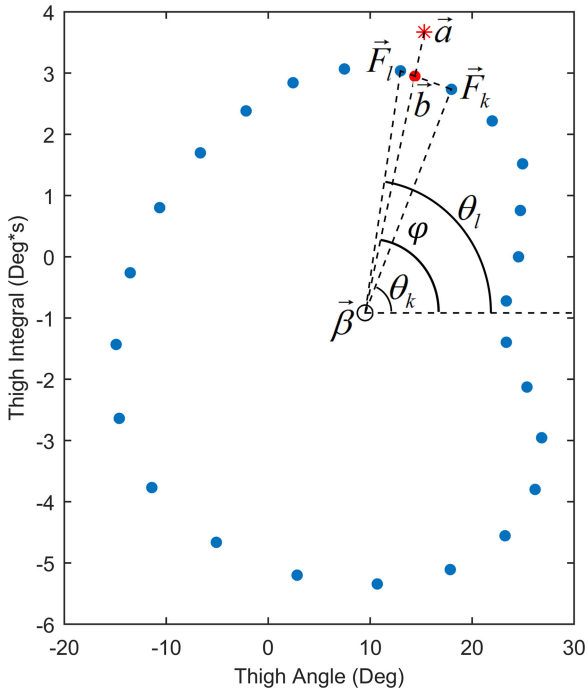

Fig. 9. Coordinate transformation example with key variables shown for clarity. Blue points represent the points in $\vec{F}$. The centroid is labeled as $\vec{\beta}$ while the point being transformed is $\vec{a}$. The angle from the horizontal to key points are also labeled as φ, θ_k, and θ_l.The point $\vec{b}$ is also indicated.

B. Factors Affecting Algorithm Efficacy

As is well known (and indicated in [21]), humans tend to adopt highly consistent movement during locomotion. Since the phase variable method classifies activity based on the nominal (i.e., mean) shape of movement, the method is particularly well-suited to applications that use non-subject-specific training. Note that using a mean-generated curve, as opposed to a distribution of points, also provides the beneficial characteristic that it avoids issues associated with overfitting, since the process of averaging by its nature precludes overfitting. An important requirement of this method, however, is that the input associated with different gait activities to be classified be characterized by a trajectory in the phase space that is qualitatively distinct (in shape and/or centroid) from that of other activities. This is in contrast with the LDA classification algorithm implemented in this study, which had no features that explicitly describe the shape of the trajectory traversed in the phase space. This lends insight into scenarios in which the LDA algorithm is expected to outperform the phase variable approach and vice versa. For example, consider the classification scenarios pictured in Fig. 8, in which two hypothetical activities have identical shapes and are centered about the same centroid (one activity is a scaled version of the other). For the PV approach, these two activities are indistinguishable from one another because the divergence rate of either activity, as calculated on the coordinate frame created by the other activity, will be close to zero. However, the standard deviation of the angle trajectory of the two activities will be different, allowing the LDA algorithm (that employs standard deviation as a feature) to distinguish between the two activities. The case pictured in Fig. 8(b) provides a counter example in which two hypothetical activities have similar means and standard deviations (in the segment angle dimension), but have different shapes in the phase space. The two activities pictured in Fig. 8(b) would therefore be easily distinguishable with the PV algorithm, but not with a typical LDA classifier (particularly one that employs mean and standard deviation as features). As such, in order for the PV algorithm to effectively classify activities, the activities should exhibit different shapes in the phase space and/or be centered about different centroids.

C. Real-Time Considerations and Possible Applications

As described here, the PV algorithm computes the RMS divergence rate associated with an entire stride for purposes of classifying activity, primarily because (1) requires the mean of the stride's limb segment angle trajectory, which is only known at the end of a stride. This type of implementation is sufficient for activity monitoring algorithms in which classification can be recorded at the end of each stride. In applications requiring classification of an activity within the span of a stride (e.g., control of a microprocessor-controlled prosthesis), the approach as implemented here would not be suitable. The algorithm proposed here, however, could potentially be adapted to smaller time windows to provide intra-stride classification functionality by employing methods similar to those described in [20].

D. Divergence Rate as a Feature for Pattern Recognition

Although presented here as a method to classify gait activities (i.e., using the vector of RMS divergence rates, and potentially supplemented with the confidence-matrix-based switching law), the divergence rate vector could separately be employed as a feature within a standard pattern recognition taxonomy. Specifically, in addition to time domain, frequency domain, or wavelet based features, a pattern recognition system could extract from the windowed data the classification vector ($\vec{C}$) as a feature, which could be used independently or in conjunction with other features as input to a classifier. Based on the study presented here, the classification vector provides an information-rich feature that encodes information about the centroid and shape of a trajectory in the phase space, which would presumably enhance the accuracy of a pattern recognition approach.

VI. Conclusion

This paper describes a method for the classification of gait activities based on representing limb motion in a phase-space-based coordinate system. The classification method as examined here utilizes the measured movement of the thigh as input, and represents this movement on a set of phase-variable-based activity-specific coordinate frames to classify an activity type. The method in essence matches a phase space trajectory to the closest "activity template," where the activity template is obtained as the average movement associated with an activity in the phase space. The process of matching is based on calculation of the curvature of a trajectory within the phase space, where zero curvature within the coordinate frame indicates a perfect match. The proposed approach was illustrated in the context of classification of three gait activities – level walking, stair descent, and stair ascent – using the thigh limb segment measured from a leg-worn IMU. The PV method outperformed an LDA classifier when used with non-subject-specific training data, while the LDA outperformed the PV when using subject-specific training data. As such, it appears that the PV method may be particularly well-suited to gait classification applications involving non-subject-specific training data.

Appendix
Coordinate Transformation

The Cartesian dimensions of a point in the classification space, $\vec{a} = [a_x, a_y]^T$, can be converted to a progression (p) and magnitude value (m) through a coordinate transformation as described in (2) (Fig. 9). In order to define this coordinate transformation, a set of points in Cartesian space, $\vec{F} = [\vec{X}, \vec{Y}]$, must be chosen from which the coordinate frame is constructed. These points represent the reference curves utilized in the main body of the paper. The centroid of the reference curve is defined by the point $\vec{\beta} = [\beta_x, \beta_y]^T$ and is given by:

$$\vec{\beta} = \left[\text{mean}\left(\vec{X}\right), \text{mean}\left(\vec{Y}\right)\right]^T \tag{8}$$

Assuming that the entries in $\vec{F}$ are linearly spaced in time, a linearly space progression vector spanning the range of $p = 0$ to $p = 1$ is created that is the length of $\vec{F}$:

$$\vec{p}_q = \frac{q - 1}{\text{length}\left(\vec{F}\right) - 1} \text{ for } q = 1 \ to \ q = \text{length}\left(\vec{F}\right) \tag{9}$$

where q indicates the qth element in $\vec{p}$. Additionally, an array of angles from the horizontal to each point in $\vec{F}$ can be found using:

$$\vec{\theta} = \text{atan2}\left(\vec{Y} - \beta_y, \vec{X} - \beta_x\right) \tag{10}$$

where *atan2*() is the four-quadrant inverse tangent function. The angle from the horizontal to the test point can also be found using this four-quadrant inverse tangent function as follows:

$$\varphi = \text{atan2}\left(a_y - \beta_y, a_x - \beta_x\right) \tag{11}$$

The angle φ is has the following bounds: ($\theta_k \leq \varphi \leq \theta_l$) where the angles θ_k and θ_l are defined by the angles from the horizontal to the points $\vec{F}_k$ and $\vec{F}_l$ where k is the kth point and l is the lth point in $\vec{F}$. The progression value of point $\vec{a}$ is found by interpolating φ between the progression values associated with the points $\vec{F}_k$ and $\vec{F}_l$ as follows:

$$p = p_k + (\varphi - \theta_k)\frac{p_l - p_k}{\theta_l - \theta_k} \tag{12}$$

where p_k and p_l are the kth and lth entries in $\vec{p}$.

To calculate the magnitude of the point $\vec{a}$, the intersection of the line that passes through $\vec{a}$ and $\vec{\beta}$ and the line that passes through $\vec{F}_k$ and $\vec{F}_l$ must be found. This intersection point, $\vec{b}$ can be quickly found as follows:

$$A = \begin{bmatrix} \frac{Y_k - Y_l}{X_k - X_l} & -1 \\ \frac{\beta_y - a_y}{\beta_x - a_x} & -1 \end{bmatrix}$$

$$B = \begin{bmatrix} \frac{Y_k - Y_l}{X_k - X_l} X_l - Y_l \\ \frac{\beta_y - a_y}{\beta_x - a_x} a_x - a_y \end{bmatrix}$$

$$\vec{b} = A^+ B \tag{13}$$

where the k or l subscript indicates the kth or lth element, respectively, of the vector indicated and where the $+$ superscript indicates the Moore-Penrose pseudoinverse. The ratio of the distances from $\vec{\beta}$ to $\vec{b}$ and from $\vec{a}$ to $\vec{\beta}$ can then be taken in order to calculate the magnitude of point $\vec{a}$:

$$m = \frac{\left\|\vec{a} - \vec{\beta}\right\|}{\left\|\vec{b} - \vec{\beta}\right\|} \tag{14}$$

Acknowledgment

The authors would like to thank R. D. Gregg for his advice regarding the phase space used in this work, and B. E. Lawson for his contributions to the methodology.

REFERENCES

[1] S. J. Preece *et al.*, "Activity identification using body-mounted sensors—A review of classification techniques," *Physiol. Meas.*, vol. 30, 2009, Art. no. R1–33.

[2] A. Avci *et al.*, "Activity recognition using inertial sensing for healthcare, wellbeing and sports applications: A survey," in *Proc. 2010 23rd Int. Conf. Archit. Comput. Syst.*, 2010, pp. 1–10.

[3] O. D. Incel *et al.*, "A review and taxonomy of activity recognition on mobile phones," *BioNanoScience*, vol. 3, pp. 145–171, 2013.

[4] S. J. Preece *et al.*, "A comparison of feature extraction methods for the classification of dynamic activities from accelerometer data," *IEEE Trans. Biomed. Eng.*, vol. 56, no. 3, pp. 871–879, Mar. 2009.

[5] H.-Y. Lau *et al.*, "Support vector machine for classification of walking conditions using miniature kinematic sensors," *Med. Biol. Eng. Comput.*, vol. 46, pp. 563–573, 2008.

[6] H. Huang *et al.*, "Continuous locomotion-mode identification for prosthetic legs based on neuromuscular–mechanical fusion," *IEEE Trans. Biomed. Eng.*, vol. 58, no. 10, pp. 2867–2875, Oct. 2011.

[7] I. C. Gyllensten and A. G. Bonomi, "Identifying types of physical activity with a single accelerometer: Evaluating laboratory-trained algorithms in daily life," *IEEE Trans. Biomed. Eng.*, vol. 58, no. 9, pp. 2656–2663, Sep. 2011.

[8] A. Mannini and A. M. Sabatini, "Gait phase detection and discrimination between walking–jogging activities using hidden Markov models applied to foot motion data from a gyroscope," *Gait Posture*, vol. 36, pp. 657–661, 2012.

[9] H. A. Varol *et al.*, "Multiclass real-time intent recognition of a powered lower limb prosthesis," *IEEE Trans. Biomed. Eng.*, vol. 57, no. 3, pp. 542–551, Mar. 2010.

[10] Y. Huang *et al.*, "A Gaussian mixture model based classification scheme for myoelectric control of powered upper limb prostheses," *IEEE Trans. Biomed. Eng.*, vol. 52, no. 11, pp. 1801–1811, Nov. 2005.

[11] A. J. Young *et al.*, "A training method for locomotion mode prediction using powered lower limb prostheses," *IEEE Trans. Neural Syst. Rehab. Eng.*, vol. 22, no. 3, pp. 671–677, May 2014.

[12] B. Chen *et al.*, "A locomotion intent prediction system based on multi-sensor fusion," *Sensors*, vol. 14, pp. 12349–12369, 2014.

[13] B. Chen *et al.*, "A new strategy for parameter optimization to improve phase-dependent locomotion mode recognition," *Neurocomputing*, vol. 149, pp. 585–593, 2015.

[14] D. J. Villarreal and R. D. Gregg, "A survey of phase variable candidates of human locomotion," in *Proc. 2014 36th Annu. Int. Conf. IEEE Eng. Med. Biol. Soc.*, 2014, pp. 4017–4021.

[15] D. J. Villarreal *et al.*, "A robust parameterization of human gait patterns across phase-shifting perturbations," *IEEE Trans. Neural Syst. Rehab. Eng.*, vol. 25, no. 3, pp. 265–278, Mar. 2017.

[16] R. D. Gregg *et al.*, "Evidence for a time-invariant phase variable in human ankle control," *PLoS ONE*, vol. 9, 2014, Art. no. e89163.

[17] M. A. Holgate *et al.*, "A novel control algorithm for wearable robotics using phase plane invariants," in *Proc. 2009 Int. Conf. IEEE Robot. Autom.*, 2009, pp. 3845–3850.

[18] R. D. Gregg and J. W. Sensinger, "Towards biomimetic virtual constraint control of a powered prosthetic leg," *IEEE Trans. Control Syst. Technol.*, vol. 22, no. 1, pp. 246–254, Jan. 2014.

[19] R. D. Gregg *et al.*, "Virtual constraint control of a powered prosthetic leg: From simulation to experiments with transfemoral amputees," *IEEE Trans. Robot.*, vol. 30, no. 6, pp. 1455–1471, Dec. 2014.

[20] D. Quintero *et al.*, "Preliminary experiments with a unified controller for a powered knee-ankle prosthetic leg across walking speeds," in *Proc. Int. Conf. IEEE Intell. Robot. Syst.*, 2016, pp. 5427–5433.

[21] D. A. Winter, *Biomechanics and Motor Control of Human Gait: Normal, Elderly and Pathological*. Waterloo, ON, Canada: Univ. Waterloo Press, 1991.